CHAPTER 54

EQUILIBRIUM PROFILES OF COARSE MATERIAL UNDER WAVE ATTACK

by E. van Hijum *)

<u>Abstract</u>. In order to obtain design criteria for artificial gravel beaches, a research programme was drawn up to study the behaviour of gravel beaches under wave attack. The present paper gives the main results of the first step in this programme, viz. the determination of the dimensions, form and way of formation of an equilibrium profile under regular, perpendicular wave attack. One of the conclusions is that gravel with a $D_{QO} < 6 \pm 10^{-3}$ m is sensitive to scale effects.

<u>1</u> Introduction. Coarse material, such as gravel and light rubble, has recently been applied in the Netherlands as a bank protection in areas exposed to wave attack. An example is the gravel beach at the Zuidwal, the southern bank of the harbour entrance to Rotterdam (Figure 1). In order to reduce the waves inside the new harbour mouth and the connected basins, a wave-damping beach is planned. In order to achieve the desired energy absorption, such a beach can consist of granular material under a small angle af inclination. For nautical and hydraulical reasons it is not possible to make the beach slope flatter than about 1:10. Such a slope can only be achieved by using gravel. Contrary to conventional types of bank protection, the prafile of a gravel layer will be deformed when exposed to wave attack. Data on the fluctuation of the profile under design wave conditions are required to ensure an adequate design. For this reason the Public Works Department of the Dutch Government charged the Delft Hydraulics Laboratory to perform investigations into the behaviour of gravel beaches under wave attack. The tests were performed in the De Voorst Laboratory of the Delft Hydraulics Laboratory.

2 Problem schematization. In solving the present problem one may follow a line as demonstrated in Figure 2. For correct profile development and longshore transport the sediment motion in the model has to fulfil the following conditions:

- the mechanism has to be the same as in the prototype
- in this mechanism scale effects have to be of such an order that they can be neglected.

Firstly the transport mechanism itself will be studied. Roughly speaking sediment transport under progressive waves will be caused by one of the types of mechanism shown in

*) Project engineer, Delft Hydraulics Laboratory, The Netherlands

COASTAL ENGINEERING

Figure 3. In this figure the groin diameter D is kept constant and the bed shear stress τ is increasing. Starting at a shear stress of zero and increasing τ the bed initially stays in a situation of rest or eventually an armoured bed. After τ has reached a critical value τ_{cr} bed load transport starts occurring. The larger grains of the grain distribution will be moved onshore and the smaller grains offshore. At increasing authe phase of ripple formation is reached. Now the mechanism of sediment transport changes completely. Under a wave crest at the lee side of a ripple an eddy is formed which picks up material from the ripple trough and from the flatter slope of the ripple. When the horizontal component of the orbital velocity decreases to zero, the eddy, still containing the material, lifts and explodes. With the following negative horizontal orbital component under the wave trough the material coming from the eddy is moved in a direction opposite to the wave direction. During this phase material is dropped on the flatter slope of the ripple and on the preceeding ripple, or it stoys in suspension, dependant of the absolute time of the wave trough and the fall velocity of the grains. The material, that stays in suspension, will be transported in positive direction under the next wave crest and will be dropped somewhere onshore. Thus, the grains with a larger diameter will move offshore and the grains with a smaller diameter onshore. This is just opposite to what happens when transport takes place as bed load only. At increasing τ a stage is reached when the ripples disappear and transport takes place as a combination of bed load and real suspended load. Next the problem of simulating these mechanisms in a model must be studied. As far as known at this moment, it is only possible to scale down the mechanism of the bed load transport, for the boundary conditions $\tau_r \tau_{ch}^{-1}$ and $\tau_v \tau_{ch}^{-1}$ (Figure 3) will not be the same in model and prototype, just as is the case with the relative ripple dimensions and the relative fall velocity of the grains. In the present model it is thus necessary to stay below the lowest value of $\tau_r \tau_{ch}^{-1}$. This seems to be a reasonable assumption for gravel. The mechanism is now known, but in this mechanism scale effects will be possible. In order to deduce these scale effects and besides to determine the profile fluctuation and the transport of gravel perpendicular to the coast, o series of tests was performed with regular perpendicular wave attack (Figure 2, step 1). Knowing which conditions are necessary to prevent these scale effects, the series of tests can be extended with three-dimensional tests, for the longshore component of the gravel transport will be on scale if the component perpendicular to the coast is on scale and the water movement is on Froudescale. In order to get a better insight into gravel movement under wave action in the prototype the present tests will have to be extended with steps 3 and 4. This paper will be restricted to the first step.

COARSE MATERIAL

3 First step: regular woves, perpendicular wave attack

3.1 Problem analysis. In describing the phenomenon of profile formation, two groups of parameters can be composed:

<u>a</u> The external parameters characterizing the wave attack and the initial beach geometry, viz. wave height and wave length on deep water (H_0 , L_0), wove period (T), depth of foreshore (h), height of beach top (k), initial slope (tg a) and grain diameter (D). Becouse of the fact that the larger grains of a grain distribution seem to be deciding for the bed load transport, for characterizing this grain distribution the D_{90} was chosen. D_{90} means that 90 $^{\circ}$ /o of the weight of a sample has a smaller diameter than D_{90} . b The internal parameters, characterizing the resulting equilibrium profile and the sediment transport during the formation of the profile. These parameters are shown in Figure 4:

h_A = height of wave run-up above the still-water level on the initial (straight) slope

h_F = height of the beach crest = height of wave run-up above the still-water level on the equilibrium profile

h_B = depth below the still-water level of the point of initial movement on the initial slope

 I_{S} and I_{K} = defining the position of the step

tg γ = gradient of the equilibrium profile at the still-water level

 β = angle of repose under water

S(y) = mean resulting sediment transport in y-direction between two points in time. The time between these points has to be much longer than the wave period.

For a correct reproduction of the external parameters in a model Froude's law of similarity has to be fulfilled, so $n_{H_O} = n_{L_O} = n_h = n_D = n_v^2 = n_c^2 = n_T^2 = n_y = n_z = n_1$, where $n_1 = (\text{length in prototype})/(\text{length in model})$, v = orbital velocity, c = phase velocity. For transmission of movement the following conditions have to be fulfilled: $n_{v2/4 \text{ gD}} = n_{CL} = n_{CM} = n_{CD} = 1$, where $\Delta = (p_s - p_w)/(p_w)$, $p_s = \text{density}$ of the sediment, $p_w = \text{density}$ of the water, $C_L = \text{lift coefficient}$, $C_M = \text{added-mass coefficient}$, $C_D = \text{drag coefficient}$. From the condition $n_v^2/_{\Delta \text{ gD}} = 1$ and Froude's law of similarity it follows that $n_A = 1$. To achieve $n_{CL} = n_{CM} = n_{CD} = 1$ the conditions given by the numbers of Reynolds, Strouhald, Keulegan- Carpenter etc. will have to be fulfilled. This is impossible. In unidirectional flow this stage will approximately be reached if the Reynolds number varies between about 10^3 and 10^5 (subcritical flow). Less is known about this subject for the case of waves, so, in order to determine possible scale effects, the way to be followed now will be to do tests with several diameters ond regard one diameter as a prototype for a smaller one.

COASTAL ENGINEERING

<u>3.2 Tests</u>. A survey of the performed tests is shown in Table 1. The choise of the external parameters was limited by three conditions:

1 The dimensions of the available wave flumes

The H-L diagram of Galvin 2, in order to stay out of the area of secondary waves 2 The condition to remain below the ripple criterion, as is shown in chapter 2 3 The combinations H-T were formed in such a way, that, concerning wave steepness, a series with constant T partly overlapped the next series with higher T. The tests with the coarsest particle diameter have been carried out in a flume with the following dimensions: length 35 m, width 5 m, depth 1.5 m. The remaining tests were done in a flume with a length of 100 m, a width of 4 m and a depth of 1 m. Starting with a straight slope the profile was sounded after 0, 3, 9, 27,... minutes of wave attack. These increasing time intervals were chosen because the profile changes in the beginning of a test were the greatest. A test was stopped when profile fluctuations becam negligible. This state of equilibrium was in the present test series reached after 0.5 - 4 hours. The soundings were made by an automatic profile follower, recorded on punched tape and processed by a computer. The mean resulting transport of gravel in y-drection in a time interval, S(y), was calculated by application of the continuity equation for the gravel between two successive soundings. Wave height and form, measured with a movable gauge of the resistance type, and orbital velocities, measured with a velocity meter of the propeller type, were recorded on paper and on tape. Sediment sorting along the equilibrium profile was determined by taking a large number of surface samples. In order to make it possible to study the water movement and grain movement in slow motion, a part of the second flume was provided with side windows and films were made of about twenty tests.

3.3 Test results. This chapter contains only the main results. More detailed information can be found in $\begin{bmatrix} 1 \\ 1 \end{bmatrix}$.

3.3.1 Profile formation. The process of profile formation is fully described by Zenkovich, Kemp and many others and can be found in $\begin{bmatrix} 1 \end{bmatrix}$, $\begin{bmatrix} 3 \end{bmatrix}$ and $\begin{bmatrix} 7 \end{bmatrix}$. A gravel beach, attacked by waves, will partly be deformed. The lower limit is fixed by the point of initial movement, the upper limit by the wave run-up on the initial profile or in the equilibrium profile. Deformation will occur until every point of the profile is in static or dynamic equilibrium. From literature it is known that two possible basic forms of the equilibrium profile exist. These two forms are indicated with several names:

942

1 summer, normal, accretion, step profile

2 winter, storm, erosion, bar profile

The first two sets of names do not say very much. The distinction that is made by the third set is dependent of the initial slope of the beach, because of the fact that the same equilibrium profile at a steep initial slope leads to erosion while at a flatter slope it might lead to accretion. Only the fourth set of names gives a clear distinction in the form of the equilibrium profile (see Figure 4). The bar-type form has a more pronounced bar in the vicinity of the breaker point. The criterion for the appearance of a bar will be given in chapter 3.3.3. The influence of the grain diameter on the profile form and profile formation is shown in Figure 5. At decreasing diameter the offshore transport of material increases at constant wave height and wave period. The same happens at constant diameter and wave period and increasing wave height. In Figure 6 the influence of the wave period is shown, and Figure 7 gives the influence of the initial slope. The initial slope does not influence the equilibrium profile, except at the connection points with the initial profile of course. In all these figures the transport lines give the mean resulting transport of gravel in y-direction in the mentioned time interval. Onshore transport is called positive.

3.3.2 Scale effects. If the material responds on scale the following conditions have to be fulfilled: $n_{hA} = n_{hF} = n_{IS} = n_{IK} = n_{hB} = n_{I}$; $n_{\chi} = n_{\beta} = 1$; $n_{S(\gamma)} = n_{I}^{2} n_{t}^{-1}$; $n_{t} = n_{I}^{\frac{1}{2}}$, where n = time scale profile formation. From the measurements of the internal parameters it appears that even for high Reynolds number the Froude law of similarity is not applicable for the two finest materials with a D_{00} of 1.8 \pm 10⁻³ m and 4.4 \pm 10⁻³ m. These two materials respond to the wave attack as if they were smaller materials. This scale effect is demonstrated in Figure 8, where the material with $D_{90} = 7.1 \pm 10^{-3}$ m is regarded as prototype. The horizontal axis shows the D_{90} and the vertical axis n_p/n_p where $n_n =$ the calculated scale of the internal parameters and $n_1 =$ the length scale of the external parameters. From this figure it can be concluded that material with $D_{90} > \sim 6.0 \pm 10^{-3}$ m responds on scale. Popov [4] found an analogous tendency. Only h_A is not influenced by scale effects. Thus it can be concluded that scale effects are restricted to the transport mechanism and do not play a role in porosity and roughness of the material in the present tests. The time scale during profile formation is deduced from the S(y) lines, and is demonstrated in Table 2. This table confirms the conclusion made above. From Figure 8 scale coefficients can be derived:

for h_B, I_K, I_S :
$$\delta_1 = \left[\frac{D_{90}}{D(\delta_1)}\right]^{\frac{1}{2}}$$
, where $D(\delta_1) = 6 \div 10^{-3}$ m; if $D_{90} \ge D(S_1)$, then $\delta_1 = 1$

$$= : \delta_2 = \left[\frac{D_{90}}{D(\delta_2)}\right]^{\frac{1}{2}}, \text{ where } D(\delta_2) = 4 \pm 10^{-3} \text{ m; if } D_{90} \ge D(\delta_2), \text{ then } \delta_2 = 1$$

3.3.3 Profile type. As stated in chapter 3.3.1 two profile types are possible, viz. step profiles and bar profiles. The criterion for appearance of a bar will, at a constant materialand water density, be a function of H_{o} , T and D_{00} and perhaps also of the initial slope. Scale effects can also play a role. The relation with H_o, T and the initial slope is studied at a constant D_{90} (= 4.4 \pm 10⁻³ m). The wave periods were 1.2, 1.6 and 2.0 seconds, the initial slopes 1:5 and 1:10. It seems reasonable to assume that the generation of a bar takes place at a certain pattern of water movement on the beach. Four characteristic moments can be distinguished in this water movement, viz. the moment of breaking (t_{α}) , the moment when the breaking wave crest reaches the mean-water level (t_1) , the moment of eliminating of the backrush velocity of the preceeding wave by the uprush velocity of the directly following wave (t_2) and the moment of maximum wave run-up (t_2) . These points were fixed by studying the films made during the tests in slow motion (factor 24). The result is shown in Figure 9. In this figure the vertical axis shows the phase difference $(t_i - t_o)/T$, with i = 0, 1, 2, 3, and the horizontal axis shows $H_o^2 L_o^{-1}$ that appears to be the governing parameter group at constant D_{90} . Of the tests with tg a = 0.2 t_0 , t_1 , t_2 and t_3 are shown, of the tests with tg a = 0.1 only t_0 and t_3 . From this figure it can be concluded that, in contrast with what is found by Kemp 3 , the phase difference between wave breaking and maximum wave run-up alone cannot be used as criterion for the change from a step to a bar profile, for, depending on $h_{breaking}/h_{B}$, the phase difference t₃/T increases with decreasing initial slope, while changing from step to bar profile occurs at the same value of $H_0^2 L_0^{-1}$. The influence of D_{90} and the scale effects in the bar-step criterion are deduced by considering all tests. This leads to the criterion $H_0^2 L_0^{-1} D_{90}^{-1} \delta_1^{-3} = 2.5$ (see Figure 10). Because of the different transport mechanisms there is no point in trying to find any agreement between this criterion and analogous criterions for sand beaches (e.g. Larras, Iwagaki, Nayak).

3.3.4 <u>Relations between internal and external parameters</u>. In an analogous way as done for the bar-step criterion governing groups of external parameters were composed for the internal parameters. These groups are shown in Table 3. Initial slope, height of beach

top and depth of forshore (if $h_{\rm R} < h$) do not influence the profile form (I_S, $h_{\rm F}$, $h_{\rm R}$, χ , β , bar/step), but only the position of the profile in horizontal direction (I_K), the time necessary until equilibrium is reached and, of course, S(y). Figure 7 shows this for the influence of the initial slope. The form of the part of the profile between beach crest and bar or step can be approached by a parabola with horizontal axis. This parabola is, just as the height of the bar, a function of $H_0 D_{90}^{-1}$. With all these relations it will now be possible to calculate and sketch the equilibrium profile for given a grain diameter and design wave conditions. This is described in detail in $\begin{bmatrix} 1 \end{bmatrix}$. In the present paper only the graphs of h_A , h_F , h_B , l_S , l_K and tg y are given. Figure 11 shows $h_A D_{90}^{-1}$ as a function of $c_0 H_0 g^{-3} D_{90}^{-3/2}$. The transport mechanism does not influence $h_A D_{90}^{-1}$ and there are no scale effects. Thus some values taken from profiles of sandy beaches given by Saville jr. [5] and Watts and Dearduff [6] are also shown in this figure. In the figures 12, 13 and 14 the relations of h_F , I_S and I_K with the governing external parameters are given. It appears that the profile type does not influence the location of the step. Figure 15 shows $h_B D_{90}^{-1}$ as a function of $H_0 D_{90}^{-1} \delta_1^{-1}$. For low waves with a low period there appears to be a dependency on the wave period too. In the insertion $h_B D_{90}^{-1}$ is given as a function of $c_0 H_0 g^{-1} D_{90}^{-3/2} \delta_1^{-3/2}$ for values of this parameter group of less than about 200. Figure 16 shows that it is possible that material is deposited below the point of initial movement. In Figure 17 the relation between tg χ and H_o D₉₀⁻¹ is given. No scale effects are found in this parameter, perhaps due to the fact that the scale effects work in the same sense on the vertical .⁻¹≈ 10. (h_R) and horizontal (I_S) parameters. A maximum value for tg χ is reached for H_a D₉₀ For very small waves with no profile formation it is abvious that to x must equal the initial slope.

<u>3.3.5</u> Optimal initial slope. For optimal design of artificial beaches it is important to known at which initial slope for given a grain diameter and design wave conditions minimum erosion and accretion will occur. Figure 7 shows that this will happen when the beach crest tends to disappear. The beach crest disappears when I_S equals I_K . With the method of least squares best fitting lines were calculated for I_S and I_K . I_S appears to equal I_K when :

$$H_0 D_{90}^{-1} \delta_1^{-1} \left\{ 1.98 - (tg a)^{-1/3} \right\} = 12.48$$

Figure 18 shows tg a as a function of $H_0 D_{90}^{-1} \delta_1^{-1}$. The optimal initial slope for a given $H_0 D_{90}^{-1} \delta_1^{-1}$ is found on or just to the right of the graph.

COASTAL ENGINEERING

3.3.6 Critical velocity. The water movement under a progressive short wave can roughly be devided into two zones, viz. an upper zone, where the water movement is hardly influenced by the bed, and a lower zone ("boundary layer") of a much smaller thickness. Figure 19 gives an idea about possible velocity profiles (component parallel to the bed) in these two layers. The maximum value in time of this component, measured just above the lower zone at the point of initial movement on the initial slope is defined here as the critical velocity. Movement of material at this point was generated when this component had its maximum value and was in all tests in positive direction. From the tests it appeared that the critical velocity at a constant grain diameter increased with the water depth. The results of one series are shown in Figure 19. Detail A gives a possible explanation: at increasing water depth and wave height the thickness of the lower zone increases too, and just outside this lower zone a higher velocity is needed to provide a grain with the same surrounding flow pattern. The critical velocity appears to reach a constant value for $h_B D_{90}^{-1} \delta_1 \approx 80$, while $v_{crit} (g D_{90})^{-\frac{1}{2}} \approx 2.0$. This phenomenon has to be kept in mind when simulating sediment movement in a pulsating water apparatus. 3.4 Limitations in use and recommendations for further research. It is clear that it is only permissible to use the obtained results within the tested range of the parameter groups. It will be interesting to know what happens at higher values of H D_{00}^{-1} and $c_{\rm c} H_{\rm o} g^{-\frac{1}{2}} D_{\rm on} -\frac{3/2}{2}$. Due to the appearance of scale effects at smaller diameters and due to the restriction to remain below the ripple criterion, wave flumes of much bigger proportions than used for the present tests will be needed.

References

- 1 Delft Hydraulics Laboratory. Reports M 1216 part 1, M 1216 part 11, M 1063 part 111, 1974
- 2 Galvin, C.J. Finite amplitude shallow water waves of periodically recurring form. CERC - note, sept. 1970
- 3 Kemp, P.H. The relationship between wave action and beach profile characteristics. Proc. 7th Conf. on Coast. Eng. 1960
- 4 Popov, I.J. Experimental research in formation by waves of stable profiles of upstream faces of earth dams and reservoir shores. Proc. 7th Conf. on Coast. Eng. 1960
- 5 Saville, J.T. Scale effects in two-dimenional beach studies. Trans. I.A.H.R., 7th Gen. Meeting, 1957
- 6 Watts, G.M. and Dearduff, R.F. Laboratory study of effect of tidal action on waveformed beach profiles. Beach Erosion Board, Techn. Mem. no. 52, 1954
- 7 Zenkovich, V.P. Processes of coastal development. Oliver and Boyd, Edinburgh and London, 1967

grain diameter	$D_{90} = 1.8 \ 4.4 \ 7.1 \ 16.5 \ (10^{-3} m)$
$(p_s = 2650 \text{ kg m}^{-3})$	$D_{50} = 1.3 \ 3.4 \ 6.1 \ 13.0 \ (10^{-3} \text{ m})$
wave height	0.037 - 0.468 (m)
wave periad	1.2 1.6 1.83 2.0 2.44 (s)
initial slape	1:5 1:10
depth af foreshare	0.25 0.40 0.50 0.80 1.00 (m)
height af beachtap	っ and still-water level

Table 1 Survey of external parameters

"protatype"	"model"	length scale	time scale
D ₉₀	D ₉₀	n n	n _t
4.4 * 10 ⁻³ m	1.8 * 10 ⁻³ m	2.44	< 1
7.1 * 10 ⁻³ m	4.4 * 10 ⁻³ m	1.61	≈1.
16.5 * 10 ⁻³ m	7.1 * 10 ⁻³ m	2.32	> 1 $(\sim n_{1}^{\frac{1}{2}})$

Table 2 Time scale during profile farmation

internal parameters	external parameters
$ \begin{array}{c} {}^{h_{B}} \delta_{1} D_{90}^{-1} \\ {}^{l_{S}} \delta_{1} D_{90}^{-1} \\ {}^{l_{K}} \delta_{1} D_{90}^{-1} \\ {}^{h_{F}} \delta_{2}^{-1} D_{90}^{-1} \\ {}^{h_{F}} \delta_{2}^{-1} D_{90}^{-1} \\ {}^{h_{A}} D_{90}^{-1} \\ {}^{\chi} \\ \beta \end{array} $	$\begin{array}{c} H_{o} \ D_{90} \ ^{-1} \\ H_{a} \ D_{90} \ ^{-1} \\ H_{a} \ D_{90} \ ^{-1} \\ H_{a} \ D_{90} \ ^{-1} \ (tga)^{-1/3} \\ (tga)^{-1/3} \\ c_{a} \ H_{o} \ g^{-\frac{1}{2}} \ D_{90} \ ^{-3/2} \\ c_{a} \ H_{o} \ g^{-\frac{1}{2}} \ D_{90} \ ^{-3/2} \ tga \\ H_{o} \ D_{90} \ ^{-1} \\ angle \ of \ repose \ under \ water \ (\sim 30^{a}) \end{array}$

Table 3 Relations between internal and external parameters

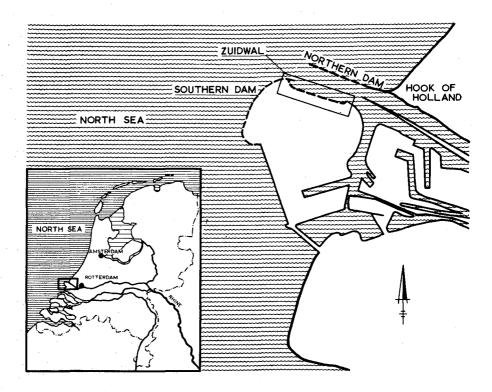


Figure 1: Situation Zuidwal

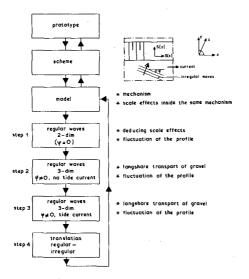


Figure 2: Problem schematization

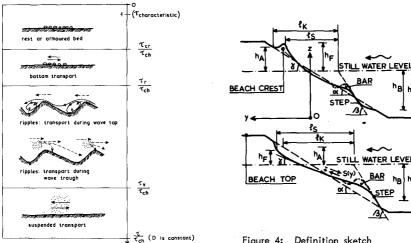


Figure 3: Transport mechanisms under waves

Figure 4: Definition sketch

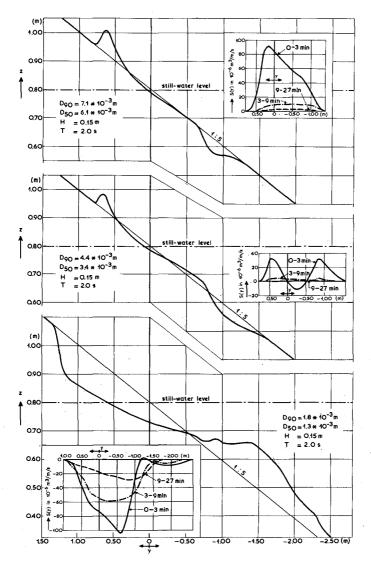
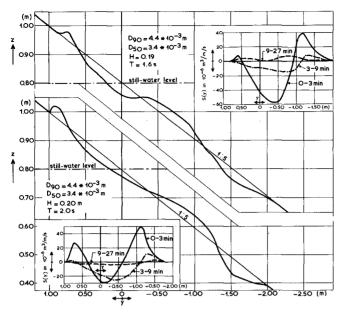


Figure 5: Influence of groin diometer





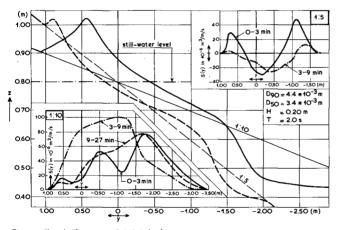
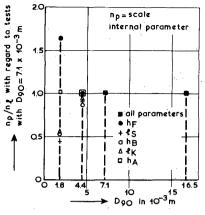
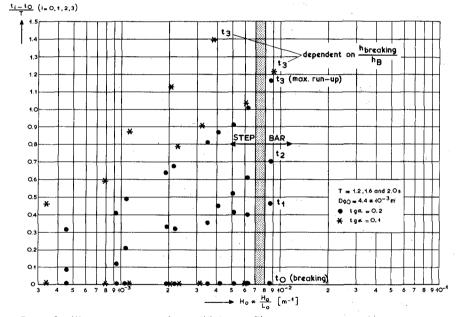
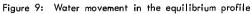


Figure 7: Influence of initial slope









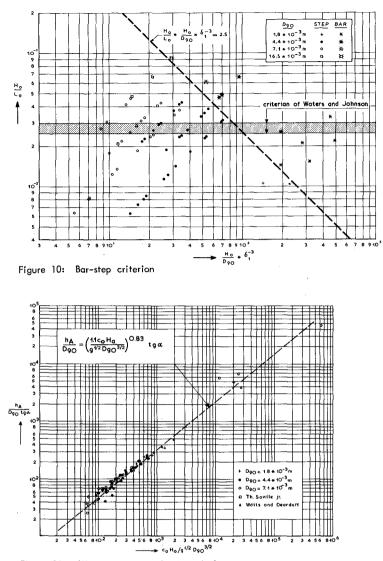


Figure 11: Wave run-up on the initial slope

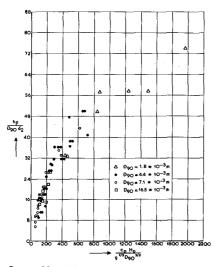


Figure 12: Wave run-up in the equilibrium profile

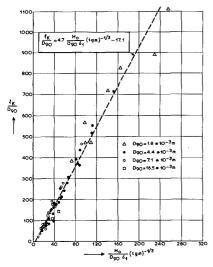


Figure 14: Location of the step

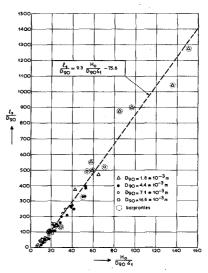


Figure 13: Location of the step

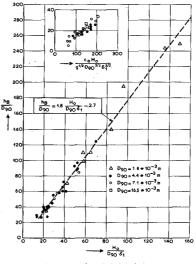


Figure 15: Depth of initial movement on the initial slope

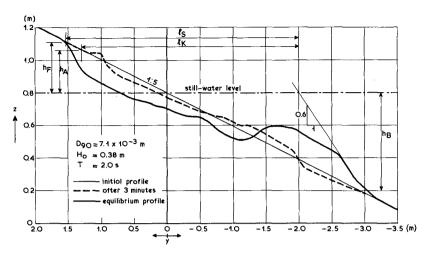


Figure 16: Deposit of moterial below the point of initial movement

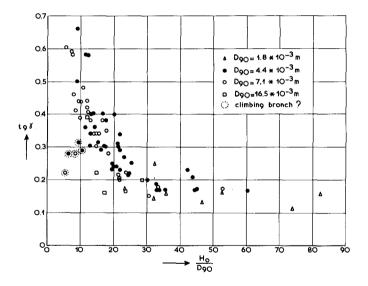


Figure 17: Slope of equilibrium profile at still-woter level

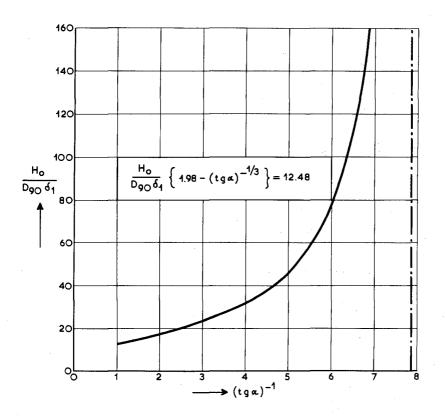
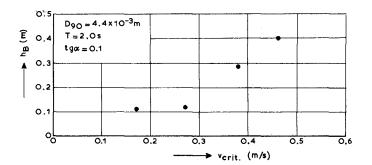


Figure 18: Disappearance af the beach crest



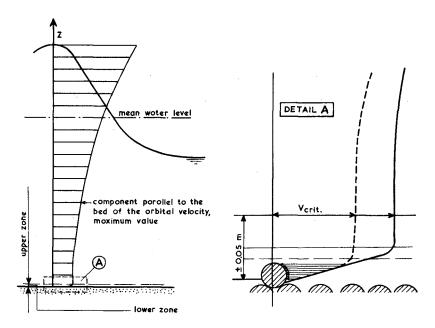


Figure 19: Criticol velocity os function of water depth